Title

Cerebral Cortex Regions Selectively Vulnerable to Radiation Dose-Dependent Atrophy.

Journal

International journal of radiation oncology, biology, physics, 97(5)

ISSN

0360-3016

Authors

Seibert, Tyler M
Karunamuni, Roshan
Kaifi, Samar
et al.

Publication Date

2017-04-01

DOI

10.1016/j.ijrobp.2017.01.005

Peer reviewed

International Journal of Radiation Oncology biology • physics

www.redjournal.org

Clinical Investigation

Cerebral Cortex Regions Selectively Vulnerable to Radiation Dose-Dependent Atrophy

Tyler M. Seibert, MD, PhD,* Roshan Karunamuni, PhD,* Samar Kaifi, MD,* Jeffrey Burkeen, MD,* Michael Connor, BS,* Anitha Priya Krishnan, PhD,† Nathan S. White, PhD,† Nikdokht Farid, MD,† Hauke Bartsch, PhD,† Vyacheslav Murzin, PhD,* Tanya T. Nguyen, PhD,‡ Vitali Moiseenko, PhD,* James B. Brewer, MD, PhD,†,§ Carrie R. McDonald, PhD,*,‡ Anders M. Dale, PhD,†,‡,§ and Jona A. Hattangadi-Gluth, MD*

*Departments of *Radiation Medicine and Applied Sciences, †Radiology, ‡Psychiatry, and §Neurosciences, University of California, San Diego, La Jolla, California*

Received Oct 12, 2016, and in revised form Dec 8, 2016. Accepted for publication Jan 1, 2017.

Summary

Neurologic deficits after brain radiation therapy typically involve decline in higher-order cognitive functions such as attention and memory rather than sensory defects or paralysis. We used quantitative magnetic resonance imaging to see whether areas of cerebral cortex involved in higher-order cognition are more vulnerable to radiation dose-

Purpose and Objectives: Neurologic deficits after brain radiation therapy (RT) typically involve decline in higher-order cognitive functions such as attention and memory rather than sensory defects or paralysis. We sought to determine whether areas of the cortex critical to cognition are selectively vulnerable to radiation dose-dependent atrophy.

Methods and Materials: We measured change in cortical thickness in 54 primary brain tumor patients who underwent fractionated, partial brain RT. The study patients underwent high-resolution, volumetric magnetic resonance imaging (T1-weighted; T2 fluid-attenuated inversion recovery, FLAIR) before RT and 1 year afterward. Semiautomated software was used to segment anatomic regions of the cerebral cortex for each patient. Cortical thickness was measured for each region before RT and 1 year afterward. Two higher-order cortical regions of interest (ROIs) were tested for association between radiation dose and cortical thinning: entorhinal (memory) and inferior parietal (attention/memory). For comparison, 2 primary cortex ROIs were also tested: pericalcarine (vision) and paracentral lobule (somatosensory/motor). Linear mixed-effects analyses were used to test

Reprint requests to: Jona A. Hattangadi-Gluth, MD, 3960 Health Sciences Dr, La Jolla, CA 92093-0865. Tel: (858) 822-6040; E-mail: jhattangadi@ucsd.edu

Presented as a preliminary version of the results in abstract form at the Annual Meeting of the American Society for Radiation Oncology, Boston, MA, Sept 25-28, 2016.

This work was partially supported by Radiological Society of North America (RSNA) Research & Education Foundation #RR1554 (TMS), National Institutes of Health (NIH) #1KL2TR001444 (JAH-G), #UL1TR000100 (JAH-G), R01NS065838 (CRM), RC2 DA29475 (AMD), and EB00790-06 (AMD); and by American Cancer Society Pilot Award ACS-IRG 70-002 (JAH-G) and American Cancer Society Research Scholar Grant RSG-15-229-01-CCE (CRM); and National Science Foundation (NSF) grant 1430082 (NSW). The content is solely the responsibility of the authors and does not necessarily represent the official views of the funding agencies.

Conflict of interest: none.

Supplementary material for this article can be found at www.redjournal.org.

Acknowledgment—The authors thank Kelly Leyden for assistance in organizing and maintaining the imaging database.

Int J Radiation Oncol Biol Phys, Vol. 97, No. 5, pp. 910–918, 2017
0360-3016/$ - see front matter
http://dx.doi.org/10.1016/j.ijrobp.2017.01.005

dependent atrophy. At 1 year after radiation therapy, higher-order association cortex regions demonstrated dose-dependent atrophy, whereas primary cortex regions did not.

all other cortical regions for significant radiation dose-dependent thickness change. Statistical significance was set at $\alpha = 0.05$ using 2-tailed tests.

Results: Cortical atrophy was significantly associated with radiation dose in the entorhinal ($P = .01$) and inferior parietal ROIs ($P = .02$). By contrast, no significant radiation dose-dependent effect was found in the primary cortex ROIs (pericalcarine and paracentral lobule). In the whole-cortex analysis, 9 regions showed significant radiation dose-dependent atrophy, including areas responsible for memory, attention, and executive function ($P \leq .002$).

Conclusions: Areas of cerebral cortex important for higher-order cognition may be most vulnerable to radiation-related atrophy. This is consistent with clinical observations that brain radiation patients experience deficits in domains of memory, executive function, and attention. Correlations of regional cortical atrophy with domain-specific cognitive functioning in prospective trials are warranted.

Introduction

Brain radiation therapy (RT) is often associated with cognitive impairment, likely mediated in part by incidental irradiation of normal brain tissue (1-3). Recent decades have seen advances in RT that provide unprecedented control and accuracy in dose delivery to therapeutic targets while minimizing exposure to normal tissues. However, although neurosurgical experience describes regions of eloquent brain to be carefully avoided (4), little is known about the regional vulnerability of the brain when it comes to RT. Current and long-standing clinical practice for fractionated RT is to consider the optic pathway, brainstem, and cranial nerves as organs at risk, whereas the brain parenchyma is treated as essentially homogeneous in terms of RT exposure risk, with only broad dose constraints to avoid overt radiation necrosis (5). There is current interest in identifying brain subregions with particular vulnerability to radiation damage as candidates for avoidance in RT planning (6, 7).

Although historically radiation damage has been thought to affect the brain's white matter rather than the cortex itself (1, 8), a recent study used quantitative magnetic resonance imaging (MRI) of glioma patients to demonstrate radiation dose-dependent cortical atrophy (9). Quantitative MRI is a well-validated technique that makes it possible to noninvasively measure the thickness of human cerebral cortex with accuracy comparable to that of postmortem histologic analysis (10-12). This technique has been successfully implemented to study the effects of age and degenerative disease, where cortical thickness has been shown to correlate with disease progression, cause, and cognitive dysfunction (13-17). There are presently no published data on variable response in humans of sublobar cortical regions to radiation dose.

Neurologic deficits observed after brain RT typically involve decline in higher cognitive functions such as attention and memory rather than more basic somatosensory defects, cortical blindness, or paralysis (1-3). This clinical observation may provide a clue to underlying radiation biology. Whereas the more basic functions are performed by the primary cortex (eg, primary visual cortex, primary motor, and primary somatosensory), it is the higher-order association cortex that is most critical for the functions of human cognition most frequently affected after RT (18). Inferior lateral parietal cortex is an area involved in a range of cognitive tasks including spatial attention and memory retrieval (19-22). The entorhinal cortex, which is the primary input source for the hippocampal formation, in turn integrates input from nearly all association cortices for its pivotal role in memory and can be considered a special case of limbic association cortex (23-25). In the present quantitative MRI study, we sought to find out whether these cortical areas subserving higher-order functions (inferior parietal and entorhinal) are selectively vulnerable to radiation-induced atrophy.

Methods and Materials

Patient cohort

This retrospective study was approved by the institutional review board. Study patients underwent fractionated (1.8-2.0 Gy per fraction) partial brain irradiation at our institution between 2010 and 2014. To be included, the patients also had to have undergone a standardized MRI protocol before receiving RT (or within the first week of RT start) and approximately 1 year after RT start (9-15 months). A cohort of 58 primary brain tumor patients was identified who met these criteria. Three of them were excluded because of poor image quality, and 1 was excluded because of large surgical resection, leaving a final cohort of 54 patients for analysis.

Forty-four of the 54 patients were treated with a total of 30 fractions. Radiation dose for the other 10 patients was converted at each location in the volume to a 30-fraction equivalent for direct comparison. Dose conversion was achieved using principles of biologically equivalent dose and an α/β ratio of 2 Gy (26, 27).

Image acquisition and preprocessing

All images were acquired using a 3T Signa Excite HDx system (GE Healthcare, Milwaukee, WI) with 8-channel

dedicated head coil. Images were acquired before start of RT (within 1 week of RT start allowed) and approximately 1 year (9-15 months) after start of RT. The standardized protocol included a 3-dimensional volumetric T1-weighted inversion recovery spoiled gradient-echo sequence (TE, 2.8 ms; TR, 6.5 ms; TI, 450 ms; voxel size $0.94 \times 0.94 \times 1.2$ mm) obtained both before and after the infusion of intravenous gadolinium contrast medium, and a 3-dimensional T2-weighted Fluid-attenuated inversion recovery (FLAIR) sequence (TE, 126 ms; TR, 6000 ms; TI, 1863 ms). All MR images were corrected for geometric distortions (28) before coregistration of the pre-RT MRI to the CT simulation images used in radiation treatment planning using custom software (9). The quality of this registration was confirmed visually slice by slice, and the resulting transformation matrix was used to resample the delivered radiation dose distribution from the treatment plan to the MRI volume space (9, 29).

Cortical thickness

Steps for cortical thickness measurement have been described previously (9, 10, 16, 30). Briefly, FreeSurfer software (http://surfer.nmr.harvard.edu; version 5.3) was used to reconstruct the cortical surface from each T1-weighted MRI volume, weighted by T2-weighted FLAIR to correct for edema or hypointensity.

The gray matter—white matter junction and the gray matter—cerebrospinal fluid (CSF) junction on MRI were each reviewed visually in a meticulous, slice-by-slice basis to identify errors in the automated estimates. This quality assurance was performed independently by 2 physicians blinded to dose distribution and was done slice by slice for the entire brain of each patient. After independent review, the 2 evaluators reached a consensus for each MRI study. Any cortical areas for a given patient where image quality or surgical changes led to segmentation error (eg, line for gray matter−CSF junction jutting out into CSF) were manually censored. Additionally, all MRI voxels falling within 5 mm of the gross tumor volume contoured by the respective treating physician at time of treatment planning were automatically excluded. The 5-mm margin accounts for uncertainty in contouring (31). The process of meticulously excluding the resection cavity and any imaging abnormality was performed independently for each time point so that any gross changes in the local anatomy were accounted for (Fig. E1; available online at www.redjournal.org).

Cortical surfaces were anatomically parcellated using FreeSurfer software and the Desikan-Killiany atlas (32) in such a manner that each patient's surface was labeled bilaterally in native space with 34 cortical regions (Fig. 1) (Fig. E2; available online at www.redjournal.org). Two of these anatomic regions (bilaterally) were selected a priori to represent higher-order association cortex: the entorhinal cortex and an area of the lateral parietal lobe designated "inferior parietal." Two additional regions were selected to represent primary cortex: pericalcarine (for primary visual) and paracentral lobule (for primary sensory/motor for the lower extremities). These 4 regions were chosen because of their described functional roles and their relatively compact geometry (to avoid large radiation dose variability across the region).

Statistical analysis

Regions of interest

Mean cortical thickness was calculated at each time point for each cortical region. Cortical thickness change over time was calculated by subtracting the mean thickness approximately 1 year after RT from the pre-RT baseline. Radiation dose data were projected onto the pre-RT cortical surface using FreeSurfer, and mean radiation dose was also calculated for each cortical region.

The relationship of mean radiation dose and mean cortical thickness change was assessed by univariate linear regression for all instances of right or left entorhinal cortex in the patient cohort (except where censored). This analysis was repeated for the other regions of interest (ROIs): inferior parietal, pericalcarine, and paracentral.

As a secondary illustration of the effect of RT dose on association cortex versus primary cortex, we also compared high-dose and low-dose exposure. All association cortex ROIs (entorhinal or inferior parietal) that received greater than 40 Gy mean dose were tested for significant cortical thickness change by the Student t test. This procedure was repeated for instances of association cortex ROIs that received less than 20 Gy, and then an unpaired t test compared the cortical thickness change in the high-dose versus the low-dose observations. A previous study had shown RT dose effects on cortex occurring above 30 Gy with standard fractionation (9), so thresholds of 40 Gy and 20 Gy were chosen a priori to ensure reasonable separation between what was categorized as high dose and low dose. The same calculations were then performed for primary cortex ROIs (pericalcarine or paracentral). Statistical significance for all tests was set at $\alpha = 0.05$ using 2-tailed tests.

Although mean radiation dose to a structure is more common in clinical practice than median dose, both dose and cortical thickness changes may be asymmetric within an ROI. Thus, we repeated the entire analysis above using median dose and median cortical thickness change.

Whole brain

After the hypothesis-driven ROI analysis described above, a secondary analysis was conducted using all 34 anatomic cortical regions in the Desikan-Killiany atlas (Fig. 1A). Consistent with the ROI analysis, the hypothesis here was that there would be a general pattern of more prominent radiation dose-dependent atrophy in anatomic regions associated with higher-order cognitive functions affected most commonly by radiation therapy.

Linear mixed-effects (LME) model analysis was performed using the R environment for statistical computing (lme4 version 1.1-7) (33). Data from the left and right

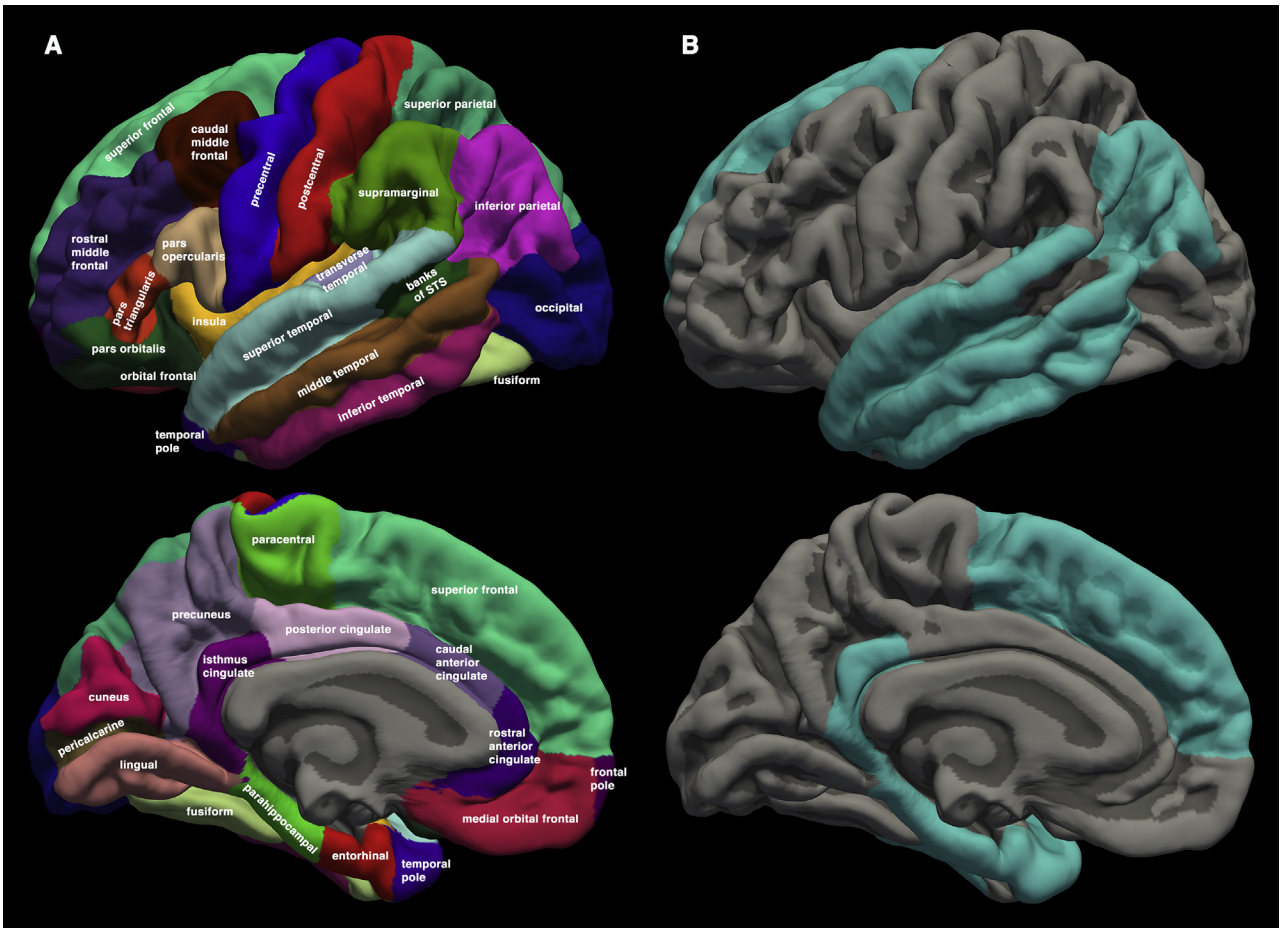

Fig. 1. (A) Cortical regions from the Desikan-Killiany atlas available in the FreeSurfer neuroimaging software suite. Regions are displayed on the FreeSurfer average brain for illustration, but statistical analyses were carried out using the corresponding regions delineated in the native magnetic resonance imaging space of each patient. Average radiation dose and average cortical thickness change were calculated for each region. (B) Cortical regions with significant radiation dose-dependent cortical atrophy in linear mixed-effects model. FreeSurfer average brain surface shown in gray (light gray for gyrus, dark gray for sulcus). Regions statistically significant after correction for multiple comparisons are colored. Only the left hemisphere is shown for convenience, but statistical tests included bilateral observations.

analogues of each cortical region were included (eg, left and right postcentral gyrus), but data from each patient were censored for tumor and surgical effects as above. Change in mean cortical thickness was chosen as the dependent variable. Inasmuch as the primary question and hypothesis related to regional variation in radiation dose response, dose (continuous variable) by region (categoric variable) interaction was included as a fixed interaction effect. Age and hemisphere (right or left) were tested as potential fixed covariates, and patient was tested as a random covariate (ie, patient-specific intercept); the addition of each of these to the model was evaluated using a likelihood ratio test, and they were included in the final LME model if $P<.05$. An estimate was calculated for the region-specific slope describing the relationship of radiation dose and cortical thickness change. To correct for multiple comparisons, the P values for these region-specific slopes (obtained based on restricted maximum likelihood) were subjected to a false discovery rate (FDR) of 0.01 (34). Regions with significant radiation dose-dependent cortical atrophy after FDR adjustment were identified. All P values were for 2-sided statistical tests.

Results

Cohort characteristics

Characteristics of the included cohort are reported in Table 1, including histologic features, sex, age, tumor location, and radiation fractionation schemes.

ROI analysis

Cortical thinning was significantly associated with mean radiation dose for the entorhinal cortex ($P=.01$) and inferior parietal cortex ($P=.02$), both association cortex ROIs. No significant association was found between radiation dose

Table 1 Patient and tumor characteristics

Characteristic	No. of patients (total = 54)	%
Sex		
Male	37	69
Female	17	31
Median age, years (range)	54 (19-77)	
Tumor histology*		
Glioblastoma, IDH wild-type	30	56
Glioblastoma, IDH mutant	2	4
Anaplastic astrocytoma, IDH wild-type	8	15
Anaplastic oligodendroglioma, IDH mutant, 1p/19q codeleted†	3	6
Anaplastic ganglioglioma	1	2
Diffuse astrocytoma, IDH wild-type	3	6
Oligodendroglioma, IDH mutant, 1p/19q codeleted†	4	7
Ganglioglioma	1	2
Pilocytic astrocytoma	1	2
Meningioma	1	2
Tumor location		
Frontal	19	35
Temporal	16	29
Parietal	2	4
Occipital	3	6
Temporoparietal	4	7
Frontoparietal	2	4
Temporoccipital	1	2
Frontotemporal	1	2
Parietooccipital	1	2
Thalamus	2	4
Cavernous sinus	1	2
Cerebellum	1	2
Surgery		
Gross total resection	23	43
Subtotal resection	25	46
Biopsy	5	9
None‡	1	2
Median time from resection to pre-RT MRI, weeks (range)	3.9 (2-20)	
Radiation therapy dose, Gy (fraction size)		
60 (2)	41	76
59.4 (1.8)	6	11
55.8 (1.8)	1	2
54 (1.8)	3	6
50.4 (1.8)	3	6
Systemic therapy		
Temozolomide§ alone	19	35
Temozolomide§ + bevacizumab	4	7
Temozolomide§ + bevacizumab + other chemotherapy‖	7	13
Temozolomide§ + other clinical trial¶	9	17
Temozolomide# + other chemotherapy**	14	26
None	1	2
Additional local therapy		
Tumor treating fields	2	4

Abbreviations: IDH = isocitrate dehydrogenase; MRI = magnetic resonance imaging; RT = radiation therapy.

* Per 2016 World Health Organization Classification of Tumors of the Central Nervous System (35).

† Combined loss of the short arm of chromosome 1 (1p) and the long arm of chromosome 19 (19q).

‡ Tumor was diagnosed as meningioma without histopathologic analysis.

§ Temozolomide given concurrently with radiation therapy for all of these patients.

‖ Carboplatin (n=5), CCNU (n=2), irinotecan (n=1), erlotinib (n=1), veliparib (n=1), buparsilib (n=1), ipilimumab (n=1), everolimus (n=1), cilengitide (given concurrently with radiation therapy) (n=1), dasatinib (n=1).

¶ Oncolytic retrovirus clinical trial (n=5), tumor antigen vaccine clinical trial (n=2), dendritic cell vaccine (n=2). Patients in this category also received CCNU (n=4), carboplatin (n=3), nilotinib (n=2), capecitabine (n=1), everolimus (n=1), palbociclib (n=1), galunisertib (n=1), irinotecan (n=1).

Temozolomide given concurrently with radiation therapy in 13 of these 14 patients.

** Lomustine (CCNU, n=9), carboplatin (n=9), irinotecan (n=4), galunisertib (n=2), nilotinib (n=2), erlotinib (n=1), palbociclib (n=1), mipsargargin (n=1), thalidomide (n=1), etoposide (n=1), trametinib (n=1), debrafinib (n=1), rapamycin (n=1), lapatinib (n=1), vemurafenib (n=1), pemetrexed (n=1).

and cortical thinning for primary visual cortex (pericalcarine; $P = .81$) or primary somatosensory/motor cortex (paracentral lobule; $P = .73$). Scatter plots are shown in Figure 2.

The Student t test results for high-dose and low-dose instances of association or primary cortex ROIs are reported in Table 2 (combining all ROIs for each category). Primary cortex ROIs showed no significant cortical thinning regardless of whether they received a high (>40 Gy) or low (<20 Gy) radiation dose. Similarly, association cortex ROIs that received a low radiation dose were not significantly atrophied compared with pre-RT baseline. However, association cortex ROIs that received >40 Gy were significantly atrophied 1 year after RT. Additionally, thickness change in high-dose association cortex was significantly greater than in low-dose association cortex.

This ROI analysis was performed again using the median for RT dose and cortical thickness changes within each region instead of mean. The results were highly similar in all respects to those described above, including all statistical tests.

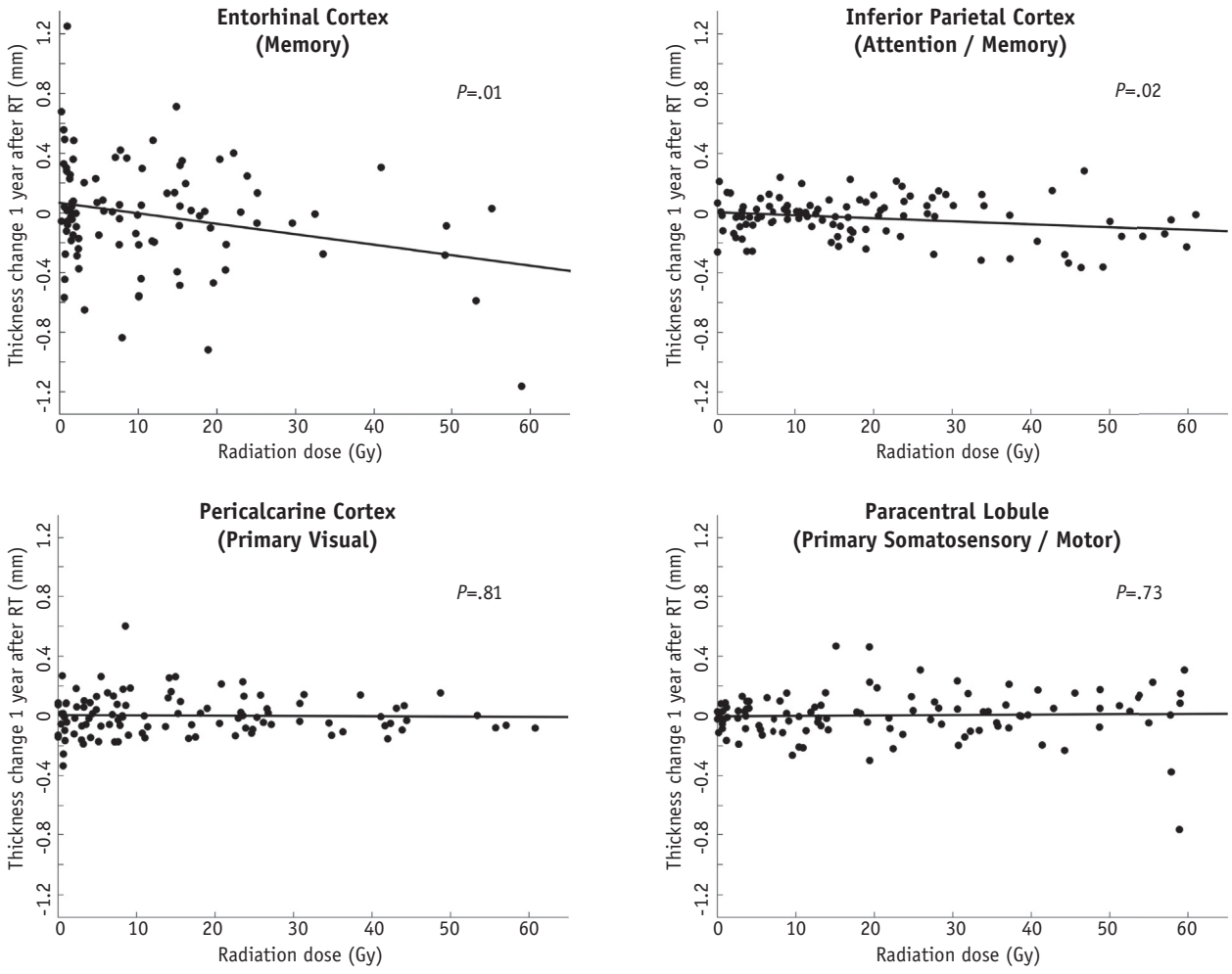

Fig. 2. Cortical thickness change versus radiation dose for 4 regions of interest. Thickness change is the mean change from preradiation baseline to approximately 1 year after start of radiation therapy. Radiation dose is the mean dose to that region of cortex. Stated (2-sided) *P* values are for the hypothesis that thickness decreases with increasing radiation dose. Regression slopes (±standard error): entorhinal −7.1 ± 2.7 μm/Gy; inferior parietal −2.0 ± 0.8 μm/Gy; pericalcarine −0.2 ± 0.9 μm/Gy; paracentral 0.3 ± 0.8 μm/Gy.

Whole-cortex analysis

All 34 cortical regions in the Desikan-Killiany atlas (Fig. 1A) were included in a linear mixed-effects model evaluating region-specific radiation dose effects on cortical thickness change. Patient age and cerebral hemisphere did not significantly contribute to prediction of cortical thinning ($P = .32$ and 0.49, respectively) and were excluded from the final model. Regions with significant radiation dose-dependent change after multiple comparisons correction (FDR<0.01) are displayed in Figure 1B. The estimated linear effect of radiation dose on cortical thickness is reported for each of these regions in Table 3. Regions failing to reach statistical significance after multiple comparison correction (gray in Fig. 1B) are reported in detail in Table E1 (available online at www.redjournal.org). Distribution of dose and thickness change for each region are reported in Table E2 (available online at www.redjournal.org).

Discussion

To our knowledge, this is the first study in humans to show selective vulnerability of specific cortical subregions to radiation dose-dependent atrophy. We found that some cortical areas involved in higher-order cognition may be more sensitive to radiation damage than areas of primary cortex.

After RT, patients are at risk for experiencing a pattern of cognitive impairment with deficits in memory, executive function, processing speed, and attention (1-3). Neurobehavioral changes are also reported (36). Given this pattern, the present study sought to determine whether regions of association cortex critical for these cognitive functions are particularly vulnerable to RT effects. To test the primary hypothesis, 2 association cortex ROIs with well-established roles in memory, attention, or both were selected to test this hypothesis: the entorhinal cortex

Table 2 Radiation dose effect on cerebral cortex regions of interest by type

Region of interest	n*	Change in cortical thickness at 1 year† (mm)	(%)	*P* value‡
Association cortex§				
High dose (>40 Gy)	20	−0.19	−6	.02‖
Low dose (<20 Gy)	142	−0.01	0	.67
Primary cortex¶				
High dose (>40 Gy)	33	−0.01	0	.80
Low dose (<20 Gy)	124	0.00	0	.87

Regions of interest were chosen a priori for hypothesis-based analysis.

* Number of observations for this category.

† Change from preradiation baseline to 1 year after start of radiation therapy.

‡ Student *t* test (2-sided) for significant cortical atrophy compared with null hypothesiss of no change.

§ Entorhinal and (lateral) inferior parietal regions (bilaterally) were selected to represent association cortex and are involved in attention and memory, cognitive functions commonly affected after brain irradiation.

‖ Also significantly greater cortical atrophy than in low-dose association cortex ($P<.01$).

¶ Primary cortex regions of interest include pericalcarine (primary visual) and paracentral (primary (somatosensory/motor for lower extremities).

(memory [23-25]) and the lateral inferior parietal cortex (attention and memory [19-22]). As hypothesized, both of these regions showed radiation dose-dependent decreases in cortical thickness approximately 1 year after RT. Association cortex ROIs whose mean dose was >40 Gy had a mean decrease in cortical thickness of 0.2 mm ($P<.01$). For context, this is more than double the rate of annual cortical atrophy in patients with Alzheimer disease (13, 37) and 10 times the rate in normal aging (38).

Table 3 Cortical thickness change per Gy (whole-cortex linear mixed-effects model)

Region	Thickness change (μm/Gy)	Standard error	*P* value*
Entorhinal	−4.8	1.1	<.0001
Inferior parietal	−2.3	0.7	.0020
Inferior temporal	−3.9	1.0	.0001
Isthmus cingulate	−1.8	0.5	.0009
Middle temporal	−3.0	0.9	.0007
Parahippocampal	−3.4	0.9	.0002
Superior frontal	−2.5	0.7	.0004
Superior temporal	−4.4	0.7	<.0001
Temporal pole	−6.5	1.0	<.0001

Regions reported here had region-specific slopes (thickness change per Gy) that were statistically significant after correction for multiple comparisons (34 regions) with a false discovery rate <0.01. All regions are reported in Table E1 (available online at www.redjournal.org).

* 2-sided *P* value from linear mixed-effects model without correction for multiple comparisons.

The radiation dose-dependent thinning measured in the association cortex ROIs can be compared with the results from the same analysis using primary cortex ROIs. Primary visual and primary somatosensory/motor regions were tested, but neither showed cortical atrophy associated with radiation dose. Even at relatively high mean dose (>40 Gy), there was no significant change in mean cortical thickness in the primary cortex ROIs. The distinction between association and primary cortex ROIs lends weight to the hypothesis that some regions of higher-order cortex are more susceptible to radiation effect, which may explain the clinical observations of functional decline in many higher cognitive processes among brain RT patients.

The whole-cortex (LME) analysis used all 34 atlas regions (Fig. 1A) and confirmed that the a priori ROIs chosen for attention and memory were among those with the strongest dose-dependent atrophy. The LME analysis also revealed additional regions that exhibited a strong association between radiation dose and cortical thinning (Fig. 1B, Table 3), all of which lie within areas of association cortex (18). The superior frontal gyrus, for example, is involved in aspects of working memory and executive functioning; both of these domains are often affected after brain RT (1-3). Although the underlying pathologic change is very likely distinct, it is also interesting that the pattern in Figure 1B is similar to that of areas most affected by Alzheimer disease, another condition leading to deficits of memory, attention, and executive function (37).

Other imaging studies provide background supporting the idea of treatment-related change in the brains of cancer patients. One recent study showed cortical thinning in 15 patients but did not address regional heterogeneity beyond lobes (9). A study of 6 brain RT patients showed lower FDG uptake 6 months after treatment in areas of brain that received higher dose (39), again without addressing regional vulnerability. Another study measured cortical thickness in 9 children with medulloblastoma who received chemotherapy and RT and found differences from their age-matched healthy peers. This cross-sectional study found differences in comparison with normal individuals, which were attributed to differential brain development, but was not designed to study RT dose dependence (40).

Previous work has suggested numerous mechanisms that might underlie radiation-induced damage to the brain and subsequent cognitive impairment, including vascular injury, decreased hippocampal neurogenesis, altered neuronal function, and neuroinflammation (41, 42). The precise details of these mechanisms, and the relative contribution each might have in cortical thickness loss after RT, are not yet fully clear (42). Nevertheless, the groundwork is laid for future studies that can comprehensively describe the connection between molecular RT changes and the macroscopic atrophy reported here.

There are several limitations to this study, including those inherent to a retrospective study of a relatively small cohort. The methods presented here are also unable to disentangle nonradiation and RT contributions to observed thickness changes. These brain tumor patients are subject to systemic therapy, tumor effects, surgical sequelae, and an unknown range of other environmental and genetic factors that may influence cortical thinning to an unknown degree. However, the analyses here specifically targeted radiation dose-dependent cortical atrophy, so even if systemic conditions or therapies played a role, it would most likely be only in potentiating the demonstrated radiation dose effect. Another limitation is the characteristics of the cohort, composed of 81% high-grade glioma patients; histologic features with more favorable prognosis could benefit the most from potential cognitive sparing RT and should be specifically included in future work. Finally, the imaging findings described here still need to be validated as a biomarker of cognitive decline through correlation with neurocognitive outcomes, as has been done with other diseases (13-17). Prospective investigation along these lines is currently under way at our institution.

After validation of cortical atrophy as a biomarker of cognitive decline, next steps in this area of research include comprehensive characterization of contributing factors beyond RT (eg, chemotherapy, surgery) and how these factors may interact with RT dose effect. We can then optimize RT plans to reduce dose to the most sensitive cortical regions and evaluate the impact of avoidance on cortical atrophy and on cognitive function. Neuroprotective agents can also be assessed for mitigation of RT effect (42).

We also intend to study the time course of cortical atrophy after RT and its relationship with the timing of neurocognitive changes.

It is concluded that areas of cerebral cortex most vulnerable to radiation-related atrophy included several regions important for higher-order cognition. This is consistent with clinical observations that brain radiation patients can experience deficits in domains of memory, executive function, and attention.

References

1. Meyers CA, Brown PD. Role and relevance of neurocognitive assessment in clinical trials of patients with CNS tumors. *J Clin Oncol* 2006;24:1305-1309.
2. McDuff SG, Taich ZJ, Lawson JD, et al. Neurocognitive assessment following whole brain radiation therapy and radiosurgery for patients with cerebral metastases. *J Neurol Neurosurg Psychiatry* 2013;84:1384-1391.
3. Saad S, Wang TJ. Neurocognitive deficits after radiation therapy for brain malignancies. *Am J Clin Oncol* 2015;38:634-640.
4. Chang EF, Clark A, Smith JS, et al. Functional mapping−guided resection of low-grade gliomas in eloquent areas of the brain: Improvement of long-term survival. *J Neurosurg* 2011;114:566-573.
5. Lawrence YR, Li XA, el Naqa I, et al. Radiation dose-volume effects in the brain. *Int J Radiat Oncol Biol Phys* 2010;76:S20-S27.
6. Gondi V, Pugh SL, Tome WA, et al. Preservation of memory with conformal avoidance of the hippocampal neural stem-cell compartment during whole-brain radiotherapy for brain metastases (RTOG 0933): A phase II multi-institutional trial. *J Clin Oncol* 2014;32:3810-3816.
7. Peiffer AM, Leyrer CM, Greene-Schloesser DM, et al. Neuroanatomical target theory as a predictive model for radiation-induced cognitive decline. *Neurology* 2013;80:747-753.
8. Asai A, Matsutani M, Kohno T, et al. Subacute brain atrophy after radiation therapy for malignant brain tumor. *Cancer* 1989;63:1962-1974.
9. Karunamuni R, Bartsch H, White NS, et al. Dose-dependent cortical thinning after partial brain irradiation in high-grade glioma. *Int J Radiat Oncol Biol Phys* 2016;94:297-304.
10. Dale AM, Fischl B, Sereno MI. Cortical surface-based analysis. I. Segmentation and surface reconstruction. *Neuroimage* 1999;9:179-194.
11. Fjell AM, Westlye LT, Amlien I, et al. High consistency of regional cortical thinning in aging across multiple samples. *Cereb Cortex* 2009;19:2001-2012.
12. Rosas HD, Liu AK, Hersch S, et al. Regional and progressive thinning of the cortical ribbon in Huntington's disease. *Neurology* 2002;58:695-701.
13. Sabuncu MR, Desikan RS, Sepulcre J, et al. The dynamics of cortical and hippocampal atrophy in Alzheimer disease. *Arch Neurol* 2011;68:1040-1048.
14. Kim YJ, Cho H, Kim YJ, et al. Apolipoprotein E4 affects topographical changes in hippocampal and cortical atrophy in Alzheimer's disease dementia: A five-year longitudinal study. *J Alzheimers Dis* 2015;44:1075-1085.
15. Wolz R, Julkunen V, Koikkalainen J, et al. Multi-method analysis of MRI images in early diagnostics of Alzheimer's disease. *PLoS One* 2011;6:e25446.
16. Du AT, Schuff N, Kramer JH, et al. Different regional patterns of cortical thinning in Alzheimer's disease and frontotemporal dementia. *Brain* 2007;130:1159-1166.
17. McDonald CR, Gharapetian L, McEvoy LK, et al. Relationship between regional atrophy rates and cognitive decline in mild cognitive impairment. *Neurobiol Aging* 2012;33:242-253.
18. Purves D, Augustine GJ, Fitzpatrick D, et al. Neuroscience. 2nd ed. Sunderland, MA: Sinauer Associates, Inc; 2001.
19. Cabeza R, Nyberg L. Imaging cognition II: An empirical review of 275 PET and fMRI studies. *J Cogn Neurosci* 2000;12:1-47.
20. Seibert TM, Gimbel SI, Hagler DJ, et al. Parietal activity in episodic retrieval measured by fMRI and MEG. *Neuroimage* 2011;55:788-793.
21. Ciaramelli E, Grady CL, Moscovitch M. Top-down and bottom-up attention to memory: A hypothesis (AtoM) on the role of the posterior parietal cortex in memory retrieval. *Neuropsychologia* 2008;46:1828-1851.
22. Olson IR, Berryhill M. Some surprising findings on the involvement of the parietal lobe in human memory. *Neurobiol Learn Mem* 2009;91:155-165.
23. Insausti R, Amaral DG, Cowan WM. The entorhinal cortex of the monkey: II. Cortical afferents. *J Comp Neurol* 1987;264:356-395.
24. Schlesiger MI, Cannova CC, Boublil BL, et al. The medial entorhinal cortex is necessary for temporal organization of hippocampal neuronal activity. *Nat Neurosci* 2015;18:1123-1132.
25. Kandel ER, Schwartz JH, Jessell TM, editors. Principles of Neural Science. 4th ed. New York: McGraw-Hill; 2000.
26. Fowler JF. The linear-quadratic formula and progress in fractionated radiotherapy. *Br J Radiol* 1989;62:679-694.
27. Bruzzaniti V, Abate A, Pedrini M, et al. IsoBED: A tool for automatic calculation of biologically equivalent fractionation schedules in radiotherapy using IMRT with a simultaneous integrated boost (SIB) technique. *J Exp Clin Cancer Res* 2011;30:52.
28. Jovicich J, Czanner S, Greve D, et al. Reliability in multi-site structural MRI studies: Effects of gradient non-linearity correction on phantom and human data. *Neuroimage* 2006;30:436-443.
29. Seibert TM, White NS, Kim GY, et al. Distortion inherent to magnetic resonance imaging can lead to geometric miss in radiosurgery planning. *Pract Radiat Oncol* 2016;6:e319-e328.

30. Fischl B, Sereno MI, Dale AM. Cortical surface-based analysis. II: Inflation, flattening, and a surface-based coordinate system. *Neuroimage* 1999;9:195-207.
31. Weltens C, Menten J, Feron M, et al. Interobserver variations in gross tumor volume delineation of brain tumors on computed tomography and impact of magnetic resonance imaging. *Radiother Oncol* 2001;60:49-59.
32. Desikan RS, Ségonne F, Fischl B, et al. An automated labeling system for subdividing the human cerebral cortex on MRI scans into gyral based regions of interest. *Neuroimage* 2006;31:968-980.
33. R Core Team. R: A Language and Environment for Statistical Computing. Vienna: R Foundation for Statistical Computing; 2015.
34. Genovese CR, Lazar NA, Nichols T. Thresholding of statistical maps in functional neuroimaging using the false discovery rate. *Neuroimage* 2002;15:870-878.
35. Louis DN, Perry A, Reifenberger G, et al. The 2016 World Health Organization Classification of Tumors of the Central Nervous System: A summary. *Acta Neuropathol* 2016;131:803-820.
36. Crossen JR, Garwood D, Glatstein E, et al. Neurobehavioral sequelae of cranial irradiation in adults: A review of radiation-induced encephalopathy. *J Clin Oncol* 1994;12:627-642.
37. Thompson PM, Hayashi KM, de Zubicaray G, et al. Dynamics of gray matter loss in Alzheimer's disease. *J Neurosci* 2003;23:994-1005.
38. Salat DH, Buckner RL, Snyder AZ, et al. Thinning of the cerebral cortex in aging. *Cereb Cortex* 2004;14:721-730.
39. Hahn CA, Zhou SM, Raynor R, et al. Dose-dependent effects of radiation therapy on cerebral blood flow, metabolism, and neurocognitive dysfunction. *Int J Radiat Oncol Biol Phys* 2009;73:1082-1087.
40. Liu AK, Marcus KJ, Fischl B, et al. Changes in cerebral cortex of children treated for medulloblastoma. *Int J Radiat Oncol Biol Phys* 2007;68:992-998.
41. Greene-Schloesser D, Robbins ME. Radiation-induced cognitive impairment: From bench to bedside. *Neuro Oncol* 2012;14:iv37-iv44.
42. Greene-Schloesser D, Moore E, Robbins ME. Molecular pathways: Radiation-induced cognitive impairment. *Clin Cancer Res* 2013;19:2294-2300.